TOPICAL REVIEW — Low-dimensional nanostructures and devices

Electrostatic field effects on three-dimensional topological insulators*

Yang Wen-Min(杨雯敏), Lin Chao-Jing(林朝镜), Liao Jian(廖 剑), and Li Yong-Qing(李永庆)†

Beijing National Laboratory for Condensed Matter Physics, Institute of Physics, Chinese Academy of Sciences, Beijing 100190, *China*

(Received 13 May 2013; revised manuscript received 7 August 2013)

Three-dimensional topological insulators are a new class of quantum matter which has interesting connections to nearly all main branches of condensed matter physics. In this article, we briefly review the advances in the field effect control of chemical potential in three-dimensional topological insulators. It is essential to the observation of many exotic quantum phenomena predicted to emerge from the topological insulators and their hybrid structures with other materials. We also describe various methods for probing the surface state transport. Some challenges in experimental study of electron transport in topological insulators will also be briefly discussed.

Keywords: topological insulator, electron transport, weak localization, surface and interface

PACS: 72.15.Rn, 73.25.+i, 03.65.Vf, 71.70.Ej **DOI:** 10.1088/1674-1056/22/9/097202

1. Introduction

Since the invention of field effect transistors by Kahng and Atalla in 1960, the gate-voltage control of material properties has been pursued intensively by the semiconductor industry and the condensed matter physics community. Electrostatic tuning of chemical potentials has played a vital role in many important experimental breakthroughs, such as the quantum Hall effect,[1] the quantum spin Hall effect,[2] and the quantum anomalous Hall effect.[3] It has also enabled physicists to observe many interesting phenomena that may lead to novel device applications. Some examples include the gate-voltage control of magnetism in magnetic semiconductors,[4] field-controlled spin precession in low-dimensional semiconductor structures,[5] electric field induced superconductor–insulator transitions,[6] as well as many other quantum phase transitions.[7]

A three-dimensional (3D) topological insulator (TI) belongs to a new state of matter that was discovered in 2007–2008.[8–12] It has an insulating bulk that can be characterized with topological invariants.[13,14] The surface of the TI is characterized by gapless states of charge carriers with a linear dispersion (i.e., Dirac particles). Unlike topologically trivial surface states formed due to band bending near semiconductor surfaces, the TI surface states are robust against disorders due to the topological protection. In addition to their fascinating intrinsic properties, topological insulators can also host many exotic quantum states when they are combined with other types of materials, such as superconductors and magnetic materials.[13–16] It is believed that the TI based hybrid structures may be useful in spintronics and topological quantum computation.

In the past five years, there has been an explosive growth in the research of topological insulators. However, most of the predicted quantum phenomena still remain to be observed presumably due to difficulties in obtaining TI materials with reasonably insulating bulk and good compatibility to other materials. The first identified TI materials, $Bi_{1-x}Sb_x$,[11,12] Bi_2Se_3, Bi_2Te_3, and Sb_2Te_3,[17–19] tend to have conducting bulks because of various defects and surface reactions to atmosphere.[20–22] This makes the clear demonstration of the surface transport a difficult task in the early days of TI research.[20,21] Thanks to enormous effort worldwide, the bulk conductivity has been reduced significantly in new TI materials or low-dimensional TI structures. The transport in the topological regime is no longer elusive in experiment.

The experimental work on reducing the bulk conductivity can be categorized into two routes. One is to use the compensation or other techniques to increase the bulk resistivity,[23–30] and the other is to use electrostatic gating to deplete the bulk carriers.[31–35] Impressive progresses have been made in both directions. In this mini-review we focus on the advances in tuning the chemical potential in topological insulators with electrostatic field effect. It can not only suppress the bulk conductivity significantly, but also shift the chemical potential across the bulk band gap, including placing the Fermi level near the Dirac point. Such gate-tuning capability is necessary for observing a number of exotic quasiparticles and quantum effects. Transport techniques for revealing the surface state transport are also reviewed. It should be noted that the main purpose of this article is to provide a brief overview of the field effect experiments on topological insulators. Readers are referred to Refs. [13], [14], and [36]–[38] for more compre-

*Project supported by the National Basic Research Program of China (Grant Nos. 2012CB921703 and 2009CB929101), the National Natural Science Foundation of China (Grant No. 91121003), and the Chinese Academy of Sciences.

†Corresponding author. E-mail: yqli@iphy.ac.cn

© 2013 Chinese Physical Society and IOP Publishing Ltd

hensive reviews of this rapid developing field.

2. Field effect control of chemical potential

As mentioned above, early experimental studies of the TI transport were complicated by the parallel conductivity in the bulk. For instance, Bi_2Se_3, often regarded as a model system for topological insulators,[17] tends to have selenium vacancies in the bulk.[23] These n-type defects are responsible for the coexistence of bulk and surface states on the Fermi level.[19] The situation is made even worse by the downward band bending near the top surface after the sample is exposed to atmosphere or even cleaved in ultrahigh vacuum.[21,22,39,40] The combined effects of the bulk donors and the surface n-doping usually place the Fermi level on the Bi_2Se_3 surface a few hundreds meV above the conduction band minimum. This is corresponding to a sheet bulk electron density on the order of 10^{13} cm^{-2} even for a 10-nm thick Bi_2Se_3 thin film.

The most commonly used dielectric oxide, SiO_2, can provide a charge tuning capability only up to about 1×10^{13} cm^{-2}. Such tunability has proven to be able to gate graphene[41] and many low-dimensional semiconductors, however it is insufficient to influence the top surface from the bottom side of a typical Bi_2Se_3 sample. As depicted in Fig. 1, the bottom-gating geometry is preferred over top-gating since it is more convenient to build hybrid structures of TI and other materials. In the case of low gate tunability, a negative gate voltage can cause a non-negligible upward band bending only near the bottom surface. In other words, the electrostatic effect from the bottom electrode is shielded by the bottom surface states and a thin bulk layer above the bottom surface. Only when the gate tunability is strong enough, or the film is sufficiently thin, the bottom gate voltage can have an impact on the top surface.[42,43]

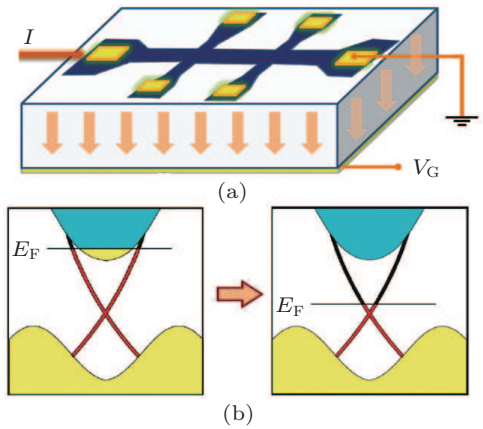


Fig. 1. (a) Schematic sketch of a topological insulator Hall bar device in a bottom-gate geometry. (b) Band diagrams of two representative transport regimes for different gate voltages. For an n-type TI sample, a negative gate voltage repels electrons from the sample and hence can lower the Fermi level E_F from the conduction band to the bulk band gap and even below the Dirac point.

2.1. Bottom-gating with $SrTiO_3$

The first effective tuning of chemical potential in 3D topological insulators was reported by Chen *et al.* in 2010.[31] In that work Bi_2Se_3 thin films were grown on $SrTiO_3$(111) substrates with molecular beam epitaxy (MBE). The high electrical breakdown strength and extremely large dielectric constant at low temperatures make $SrTiO_3$ an excellent dielectric material for bottom-gating of Bi_2Se_3. Charge tunability exceeding 2×10^{13} cm^{-2} can be readily achieved with gate voltages less than 200 V, even though careful preparation of the $SrTiO_3$ surface is necessary to obtain single crystalline films with smooth surface morphology and also to maintain the high dielectric strength of the substrate.[44]

Figure 2 shows the basic transport properties of a 10-nm thick Bi_2Se_3 thin film grown on $SrTiO_3$ substrate. At zero gate voltage, i.e., $V_G = 0$ V, the Hall resistance indicates n-type transport with a sheet electron density larger than 2×10^{13} cm^{-2}. Upon applying a negative V_G, the Hall coefficient R_H starts to increase as a consequence of decreasing electron density. At $V_G = -86$ V, a maximum in R_H is reached. When V_G becomes more negative, the sign of R_H is reversed, suggesting that holes participate in the transport. The strong nonlinearity in the Hall resistance curve indicates the coexistence of multiple types of carriers at large negative gate voltages. A simple qualitative analysis based on the two-band model points to the ambipolar transport. In this regime both electrons and holes contribute significantly in the transport and the longitudinal resistance R_{xx} is greatly enhanced. The R_{xx} maximum shows up at a gate voltage more negative than that for the R_H maximum. In monolayer graphene, the R_{xx} maximum can be regarded as an evidence for the Fermi level passing the Dirac point, and the transport is characterized by the coexistence of electron and hole puddles due to disorders. In the one-side gated TI sample, however, the R_{xx} maximum may have different meaning because of the gradient in electrostatic potential. The magnitude of the gradient is determined by many factors, including the strength of the external electric field, the doping level in the bulk, the interfacial density of states near the bottom surface, as well as doping of the top surface due to exposure to atmosphere or reaction with the capping layer. In principle, the band diagram can be determined by solving the classical 1D Poisson equation if these details are known and the quantum confinement effect can be neglected. Nevertheless, we could state qualitatively that, in case of sufficiently large electrostatic potential gradient and weak disorder, the TI thin film may separate into two conducting channels, an n-type channel on the top and a p-type one near the bottom surface (interface).

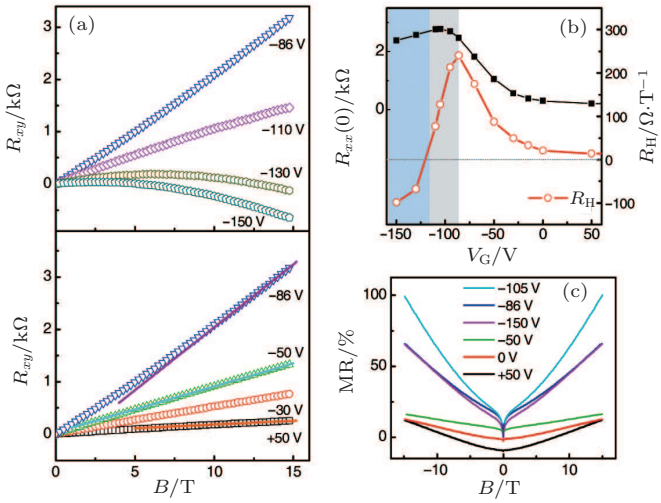


Fig. 2. Transport properties of a 10-nm thick Bi_2Se_3 film grown on $SrTiO_3(111)$ substrate at magnetic fields up to $B = 15$ T. (a) Hall resistance (R_{xy}) curves at various gate voltages. (b) Gate-voltage dependencies of the Hall coefficient R_H and the longitudinal resistivity R_{xx} at $B = 0$, i.e., $R_{xx}(0)$. The signs of R_H and R_{xy} are set to positive and negative for electrons and holes, respectively. (c) Magnetoresistance (MR) at various gate voltages. It is defined as MR $= [R_{xx}(B)/R_{xx}(0) - 1] \times 100\%$.[44]

Other TI thin films, including Bi_2Te_3, Sb_2Te_3, and $(Bi_{1-x}Sb_x)_2Te_3$, can also be grown on $SrTiO_3(111)$ substrates with MBE,[35] since they have the same crystalline structure as Bi_2Se_3. Undoped Bi_2Te_3 is usually n-type due to the Te vacancies, whereas the Sb–Te antisites make Sb_2Te_3 films p-type. The compensation effect between these two types of defects makes the ternary compound $(Bi_{1-x}Sb_x)_2Te_3$ an attractive system to obtain more insulating bulk by optimizing the Bi–Sb composition.[27,28] The thermally activated transport has indeed been observed for $x \approx 0.5$ from room temperature down to $T \approx 50$–100 K.[27,28,35] This is quite different from the monotonic decrease of resistivity with decreasing T for Bi_2Se_3, Bi_2Te_3, and Sb_2Te_3 thin films over the same temperature range. Due to the much reduced bulk carrier density in $(Bi,Sb)_2Te_3$ thin films, the ambipolar transport can be obtained more consistently than that in Bi_2Se_3 thin films with bottom-gating. Figure 3 shows the transport data for a 20-nm thick $(Bi,Sb)_2Te_3$ film with $x \approx 0.5$. In addition to the maxima in R_H and R_{xx}, a minimum in R_H appears at $V_G = -105$ V. For gate voltages between the two extrema in R_H, the transport is in the ambipolar regime, while for gate voltages outside this region, the transport is dominated by either electrons or holes. This suggests that the Fermi level can be tuned from the conduction band to the valence band for the entire thickness. Such a full range tuning of chemical potential has never been achieved in Bi_2Se_3 thin films with a single gate. Recently, similar tuning of chemical potential in Cr doped $(Bi,Sb)_2Te_3$ thin films grown on $SrTiO_3$ has allowed the observation of the quantum anomalous Hall effect.[3] In that work, the chemical potential was tuned into an energy gap opened by the perpendicular magnetic order.

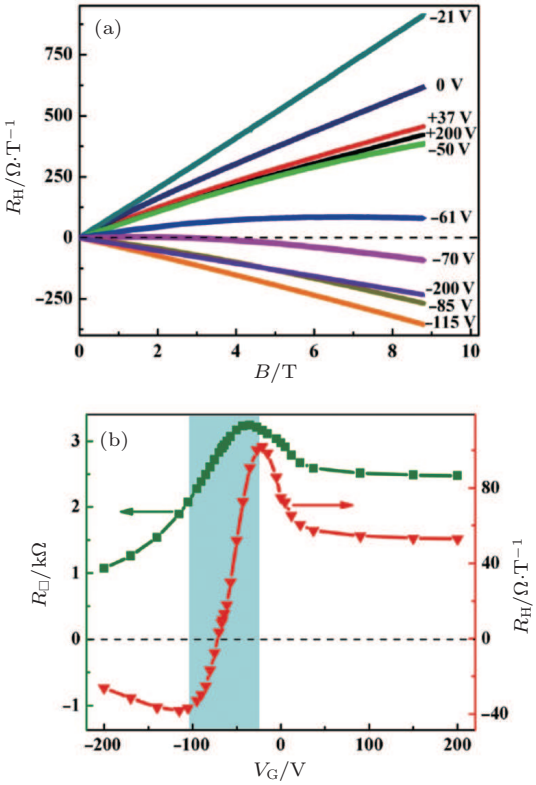


Fig. 3. Transport properties of a 20-nm thick $(Bi,Sb)_2Te_3$ film grown on an $SrTiO_3$ substrate at magnetic fields up to $B = 9$ T. (a) Gate-voltage dependencies of the Hall resistance curves show that the dominated charge carriers in the entire sample can be tuned from electrons to holes by one-side gating. (b) Gate-voltage dependencies of the longitudinal resistance per square and the Hall coefficient suggest that the Fermi level can be tuned from conduction band to valance band. The sign of R_H is set to positive for electrons.[35]

The drawback of $SrTiO_3$ is that the large gating effects are only available at low temperatures since its capacitance has a Curie law type of temperature dependence.[45] The nonlinear electric field dependence of the capacitance also requires extra measurements in order to obtain the actual change in the charge density. Trap states at the TI/$SrTiO_3$ interface also complicate the characterization of the electronic structure, as well as pose limitations in high speed device applications.[46] In contrast, such difficulties can be circumvented by using SiO_2 dielectric layers on Si substrates. However, SiO_2 is not suitable for the epitaxial growth of large area, single crystalline TI thin films due to its amorphous nature.

2.2. Bottom-gating with SiO_2

A lot of work has been carried out to tune the chemical potential in Bi_2Se_3 structures with SiO_2/Si bottom gating. It has been applied to study either microflakes cleaved from single crystals[32,34,47,48] or microplates grown with chemical vapor deposition or other methods.[49] In many cases, the field effect can only deplete a thin layer of bulk electrons near the bottom surface of Bi_2Se_3, resulting in very modest suppression of bulk conductivity.[47,48] Such difficulty cannot be attributed to the high density of n-type de-

fects in the bulk alone. For instance, the sheet carrier density corresponding to a 10-nm thick microflake cleaved from a Bi_2Se_3 single crystal with $n_e = 1 \times 10^{17}$ cm^{-3} is only 1×10^{12} cm^{-2}, which would be removed by gating fairly easily. The exposure of the Bi_2Se_3 surface to atmosphere during the device fabrication could be a main source for the large density of excess electrons.[21,22] A nice technique to solve this problem is to deposit acceptor-type 2,3,5,6-tetrafluoro-7,7,8,8-tetracyanoquinodimethane (F4TCNQ) molecules onto the TI surface (see Fig. 4).[34] It was previously applied to graphene by Coletti *et al.*,[50] and a significant hole-doping effect was obtained due to the large electron affinity of F4TCNQ molecules. With the combination of SiO_2/Si bottom-gating and molecular doping on the top surface, Kim *et al.* managed to achieve full range tuning of chemical potential in Bi_2Se_3 microflakes.[34] Since the starting Bi_2Se_3 crystal has a very low bulk electron density ($n_e = 1 \times 10^{17}$ cm^{-3}), it was argued that the chemical potential can be tuned nearly symmetrically on the top and bottom surfaces with a single gate.[34] Following the same hybrid tuning scheme of chemical potential, Cho *et al.* recently studied the superconducting proximity effect in Sb doped Bi_2Se_3 thin flakes in a regime with dominant surface transport.[51]

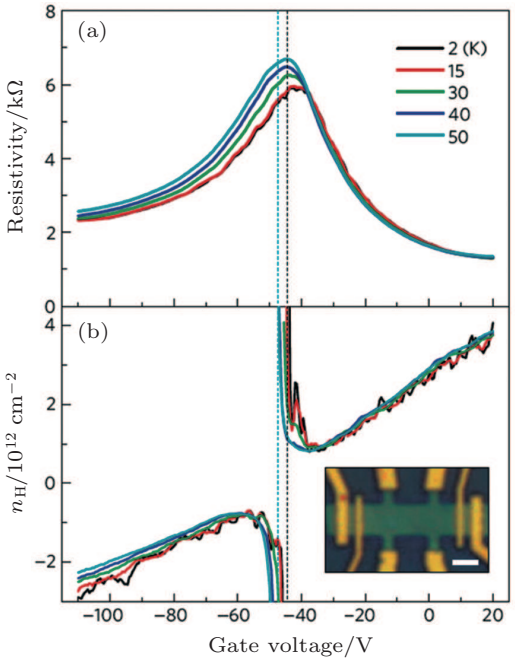


Fig. 4. Tuning the chemical potential in an F4TCNQ-doped Bi_2Se_3 microflake with an SiO_2/Si back-gate. (a) Gate-voltage dependence of the longitudinal resistivity. (b) Gate-voltage dependence of the carrier density n_H extracted from the Hall measurements. The sign of n_H is set to positive for electrons.[34]

While significant tuning of chemical potential in Bi_2Se_3 is usually difficult to achieve with bottom gating, many groups have reported large gating effects on Bi_2Te_3,[52,53] $(Bi,Sb)_2Te_3$,[28,35] $Bi_2(Se_xTe_{1-x})_3$,[54,55] $(Bi,Sb)_2Se_3$,[56] and $(Bi,Sb)_2(Te,Se)_3$ thin flakes or nanoplates.[57–59] This may be attributed to different surface chemistry upon exposure to atmosphere, as well as low bulk carrier densities due to the compensation effects in the ternary and quaternary TI compounds.

2.3. Top-gating with oxides and ionic liquids

Even though the progresses on bottom-gating mentioned above have laid foundation for many interesting experiments on topological insulators, efforts on top-gating of topological insulators are also noteworthy. A large gating effect on Bi_2Se_3 thin films was demonstrated by Steinberg *et al.* with HfO_2 as a top-gate dielectric.[60] Both the R_{xx} maximum and the reversal of sign of R_H have been observed in 20-nm thick microflakes. Similarly, Al_2O_3 grown with atomic layer deposition was also shown to be able to provide strong tunability for TI thin films.[61] An advantage of the top-gating is that the oxide dielectric can be defined on the nanometer scale with lithographic techniques. Such spatial selectivity in gating is indispensible in some experimental proposals, such as topological p–n junctions.[62]

Another interesting top-gating technique is based on electrolytes.[63,64] Under the influence of the gate electrode, a high density layer of anions or cations are accumulated on the top of the sample surface. It can provide charge tuning capability up to 1×10^{15} cm^{-2}, at least one order of magnitude higher than that of any known oxide dielectric. This liquid-gating technique remains valid at liquid helium temperatures. However, the electrolyte has to be warmed up to much higher temperatures when the gate voltage needs to be changed. Despite such inconvenience, it has been applied to study many types of materials, allowing for the observation of some interesting phenomena, such as the superconductor–insulator transition in $SrTiO_3$.[65] Subsequent to the work of Yuan *et al.* on Bi_2Te_3 thin films,[66] this technique has also been used to gate Bi_2Se_3[32] and $(Bi,Sb)_2Te_3$ thin films,[67] as well as $Bi_{2-x}Sb_xTe_{3-y}Se_y$ bulk crystals.[68] The ambipolar transport were obtained in all cases. It should be noted, however, that the gating technique based on ionic liquids is also not convenient for high speed applications.

3. Probing surface states with quantum transport properties

Observation of gate voltage induced R_{xx} maximum and R_H extrema is a necessary condition for the study of intrinsic transport properties of the surface states in many topological insulators. However, such ambipolar transport features cannot ensure the transport is truly in the topological regime, since similar behaviors can also appear in narrow band semiconductors with topologically trivial surface states or even without the surface states. Moreover, angular resolved photoemission spectroscopy (ARPES) experiments revealed that quantum well states with a parabolic dispersion can form near the

TI surface due to downward band bending.[39,69] It is impossible to differentiate such surface-accumulated 2D electron system from those of Dirac nature solely based on the basic transport features discussed in the previous section.

Up to now the ARPES experiments have played a dominant role in confirming whether a material is a topological insulator, even though the TI surface states are expected to have many interesting quantum transport properties associated with the π Berry phase due to the spin-momentum locking.[70] Most of the difficulty can be attributed to the fact that TI materials with reasonably insulating bulk are difficult to obtain, especially during the early days of TI research. During the past few years, the enormous amount of experiment effort has resulted in a remarkable improvement in the quality of TI materials. Some subtleties in interpreting the transport data have also been clarified. Now it is possible to unveil the TI surface states with quantum transport, even though caution has to be taken during the analysis of the transport data because of a number of complications, which are discussed below.

3.1. Shubnikov–de Haas oscillations

Shubnikov–de Haas (SdH) oscillations are periodic changes in longitudinal conductance G_{xx} due to the quantized motion of electrons in magnetic fields.[71] The SdH oscillations are described by

$$\Delta G_{xx} \propto \cos\left[2\pi\left(\frac{F}{B}+\beta\right)\right], \tag{1}$$

where $F = \frac{1}{\Delta(1/B)} = \frac{S_F}{4\pi^2}\frac{h}{e}$ is the frequency of oscillations with $1/B$ periodicity. For a 3D system, S_F is the extremal area of the cross-section of the Fermi surface perpendicular to magnetic field $\boldsymbol{B}$. In two dimensions, S_F is reduced to the area enclosed by the Fermi circle. It is therefore possible to differentiate a 3D electron system from a 2D one by performing measurements in tilted magnetic fields. For a 2D system, the SdH oscillations are only dependent on the perpendicular component of the B field (with oscillation frequency $F \propto 1/\cos\theta$), whereas in 3D, the angular dependence of F is determined by the shape of the Fermi surface.

Tilted field measurements of SdH oscillations in topological insulators (e.g., Bi_2Se_3) can be dated back to early 1970s.[72] Observations of SdH oscillations with 2D characteristics were reported only after they were identified as topological insulators in 2009.[73–75] The angular dependence of the oscillation frequency alone is however not sufficient to confirm the existence of nontrivial topological order, because similar behavior is also expected for a 2D electron system with a parabolic dispersion, which could exist near the surface due to band bending effects.[39,69]

The phase factor β in Eq. (1) can in principle be used to tell whether the transport is of Dirac nature. It is given by $\beta = 1/2 - \Gamma(C)/2\pi$, where $\Gamma(C)$ is the Berry phase of a closed loop C.[76] The phase β takes a value of 1/2 for electrons in a parabolic band, while for a linear dispersion, the π Berry phase leads to $\beta = 0$. Historically speaking, the π Berry phase of Dirac electrons was first demonstrated in transport measurements of graphene.[77,78] In experiment, β can be extracted by plotting $1/B_n$ as a function of n. Here $1/B_n$ is the value of $1/B$ corresponding to the G_{xx} minimum of the n-th Landau level, which satisfies $F/B_n + \beta = n + 1/2$. For graphene, $\beta = 0$ can be determined from experiments with high accuracy. Figure 5 shows similar results obtained from a $BiTe_2Se$ single crystal with large bulk resistivity.[79]

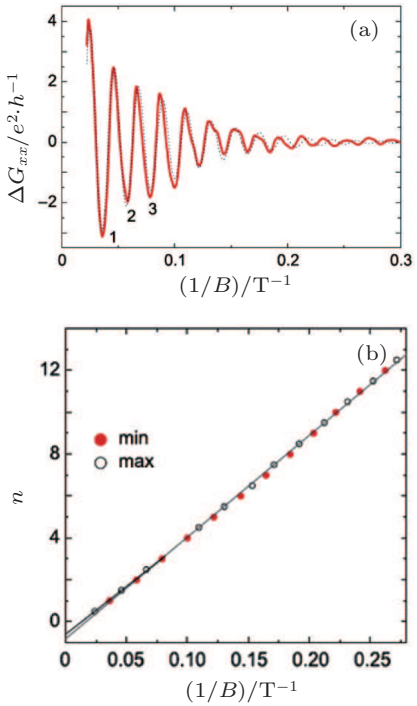


Fig. 5. Probing the Berry phase of the surface states of a Bi_2Te_2Se single crystal with Shubnikov–de Haas oscillations. (a) The oscillatory part of the longitudinal conductance, ΔG_{xx}, plotted as a function of the inverse of magnetic field $1/B$. (b) Landau level index plot of the SdH oscillations. The best linear fit gives a Fermi cross-section area S_F of 48.5 T. The straight line extrapolate produces an intercept of -0.61 ± 0.03 on the n axis, close to $\gamma = \beta - 1/2 = -1/2$ expected for the surface Dirac fermions.[79]

In the literature, the values of β obtained from the SdH measurements of topological insulators are however quite scattered due to the following reasons.[80] First, many measurements were performed on samples with significant bulk conductivity, which leads to incorrect indexing of the SdH oscillations by using R_{xx} minima, even though such practice is often justified for graphene or GaAs based 2D electron systems. Second, the dispersion of the TI surface states is not perfectly linear. The broken particle–hole symmetry can also lead to β deviating from that for the π Berry phase in some circumstances.[80] Third, the mobilities of TI samples are still much lower than graphene. This forces the measurements being carried out in high magnetic fields. The Zeeman correction

may also complicate the data analysis, even though the g factor of the surface states might be much smaller than that of the bulk carriers.[79,81] Finally, the 2D electron system with a parabolic dispersion accumulated near the surface may also give rise to SdH oscillations. It is argued by Bansal *et al.* that the 2D electron system in the surface accumulation layer may have high mobility than the surface Dirac fermions based on the two-band fittings of nonlinear Hall resistances.[82] As noted by Ando in a recent review,[38] caution is also needed in analyzing the transport with the two-band model, since the parameters extracted from the Hall resistance data often fail to describe the longitudinal resistance in the same sample. Indeed, the linear magnetoresistance observed in many TI samples[35,44,83–85] defies the description based on the classical two-band model.[82] Further work is needed in order to account for these discrepancies.

3.2. Low field magnetoresistance due to weak antilocalization

Although SdH oscillations allow for the determination of the Berry phase, the application of this technique is limited to high magnetic fields (usually $B > 5$ T) due to low carrier mobilities in most known topological insulators. Moreover, SdH oscillations cannot be observed in many TI samples, particularly in TI thin films, which are more important for device applications than bulk samples. Fortunately, the π Berry phase of the TI surface states can be manifested in a different manner, namely, the weak antilocalization effect near zero magnetic fields. This serves as the basis of an alternative method for revealing the surface state transport.[31,32]

At low temperatures, electrons can remain phase-coherent after many elastic scattering events. If the spin–orbit coupling (SOC) is negligible, the constructive interference between the pair of time-reversed closed paths results in the enhancement of backscattering and increase in resistivity in comparison to the classical transport. This is the weak localization (WL) effect, which has been studied for three decades.[86] The π Berry phase of the TI surface states leads to an opposite effect, namely, the weak antilocalization (WAL) due to the suppression of backscattering.[31,87] Applying a perpendicular magnetic field breaks the time-reversal symmetry, causing negative and positive magnetoresistance for WL and WAL, respectively. This can also be understood as a consequence of the ensemble average of the Aharonov–Bohm phases exerted onto various electron paths by the magnetic field.[86] The magnetoconductivity (MC), defined as $\Delta\sigma_{xx}(B) = \sigma_{xx}(B) - \sigma_{xx}(0)$, namely, the quantum correction to conductivity due to WL and WAL, can be written in the following form:

$$\Delta\sigma_{xx}(B) \simeq \alpha \frac{-e^2}{2\pi^2\hbar}\left[\psi\left(\frac{1}{2}+\frac{B_\phi}{B}\right) - \ln\left(\frac{B_\phi}{B}\right)\right], \quad (2)$$

where $\alpha = -1$ and $1/2$ respectively for WL and WAL in a 2D electron system without valley degeneracy. Here $\psi(z)$ is the digamma function, $B_\phi = h/(4el_\phi^2)$ is the dephasing field, and l_ϕ is the dephasing length.

In the case of WAL, equation (2) can be regarded as the strong SOC limit of the Hikami–Larkin–Nagaoka equation, which describes the MC of a traditional 2D system with non-negligible SOC.[86,88] In other words, the bulk layer in a TI thin film would also be described by Eq. (2) with $\alpha = 1/2$ since the SOC is usually very strong in most TI materials. Therefore, the MC with $\alpha = 1/2$ cannot be treated as a sufficient evidence for the π Berry phase of the surface states. Instead, α values larger than 1/2 are expected for TI thin films with insulating bulk. If the top and bottom surfaces can be tuned to have the same dephasing length and the coupling between them is negligible, one would expect identical contributions from two independent channels, and $\alpha = 2 \times 1/2 = 1$. Therefore, a smoking gun for the transport in the topological regime would be the observation of $\alpha = 1$ and deviation from this value upon gate tuning.

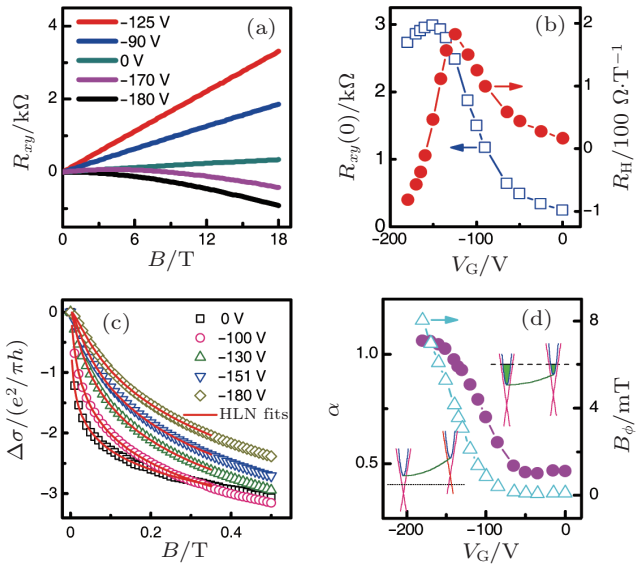


Fig. 6. Magnetotransport properties of a 10-nm thick Bi_2Se_3 thin film with large gate-tunability. (a) Gate-voltage dependence Hall resistance R_{xy} up to $B = 18$ T. (b) Gate-voltage dependence of longitudinal resistance R_{xx} at $B = 0$ and Hall coefficient R_H. The sign of R_H is set to positive and negative for electrons and holes, respectively. (c) Magnetoconductivity data (symbols) and fits to Eq. (2) (lines) at various gate voltages. (d) Gate-voltage dependencies of α and B_ϕ obtained from the fits to Eq. (2). Insets show the sketches of the band diagrams of two different transport regimes. The top (bottom) surface is depicted on the left (right). The gate voltage is applied with a gate electrode deposited on the bottom of the $SrTiO_3$ substrate.[89]

A clear demonstration of gate voltage tuned WAL was reported by Chen *et al.*, who measured Bi_2Se_3 thin films over a large range of carrier densities and mobilities.[89] It was found that when the Fermi level is located above the bulk conduction band minimum, α is close to $1/2$. In this case, the surface and bulk transport channels coexist. The observation of $1/2$ can

be attributed to strong surface-bulk scatterings, which cause the sample behaving like a single channel system.[90] When a large negative gate voltage is applied, a depletion layer in the bulk develops and separates the electron system into two relatively independent channels on the top and bottom of the sample. This is manifested as α close to 1 at large negative gate voltages,[89] as shown in Fig. 6.

In addition to the work on Bi_2Se_3,[32,60,89,91] the deviation of α from 1/2 has also been observed in other TI thin films.[53,54,92] These results are often explained with the two-channel transport model, in which the upper limit of α is 1. However, recent experiments also showed that α considerably larger than 1 can also be extracted from low field magnetoconductivity data.[59] This indicates that an extra channel or another source of magnetoconductivity may exist in the sample. Independent methods for detecting the hidden channels or mechanisms for magnetoconductivity are highly desirable in order to gain further insight into the topological insulators. Recent work on parallel field magentotransport by Lin *et al.* provides a promising route to tackle such a challenging problem.[93]

3.3. Quantum oscillations due to phase coherent transport

The Aharonov–Bohm (AB) phase can also be manifested in quasi-1D structures. Altshuler, Aronov, and Spivak (AAS) predicted in 1981 that magnetic fields applied parallel to a hollow metallic cylinder (with cross-section area S) can lead to conductance oscillations with a B period proportional to $\Phi_0/(2S)$,[94] with $\Phi_0 = h/e$ denoting the flux quantum. This effect was first observed by Sharvin *et al.* with a glass fiber coated with Mg thin film.[95] Another beautiful demonstration of the AAS effect was made in parallel field measurements of multiwall carbon nanotubes.[96] The $h/2e$ periodic oscillations can be understood as the AB phase difference between the time-reversed loops around the quasi-1D structures, i.e., $2\pi(2BS/\Phi_0) = 2\pi(2\Phi/\Phi_0)$. For an electron system with weak SOC, the conductance minima appear at integer or half integer magnetic flux quanta ($\Phi = n\Phi_0/2$, $n = 0, 1, 2, \ldots$) because of the constructive interference. For TI surface states, the π Berry phase is expected to result in an opposite effect, namely, the $h/2e$ oscillations with conductance maxima located at integer or half-integer magnetic flux quanta. However, this statement is only true when the transport is in the diffusive regime.[37] In the case of ballistic transport, oscillations may become h/e periodic, with the maxima located either at integer or half-integer flux quanta according to recent theoretical studies.[97,98]

The first experimental work on quasi-1D TI systems was carried out by Peng *et al.* on Bi_2Se_3 nanobibbons.[99] They only observed h/e oscillations with conductance maxima located at integer magnetic fluxes. Subsequently, similar measurements were extended to other TI nanostructures, such as Bi_2Te_3[52,100,101] and Ag_2Te[102] nanoribbons, and both h/e and $h/2e$ oscillations have been observed. In particular, Hong *et al.* recently reported that by combining surface engineering and electrostatic gating, the transport in Bi_2Se_3 nanoribbons can be tuned from ballistic to diffusive regime and correspondingly the relative magnitude of h/e to $h/2e$ oscillations can be varied in a controlled manner (see Fig. 7).[103] This is consistent with the theories in Refs. [97] and [98], which are summarized in a recent review by Bardarson and Moore.[37]

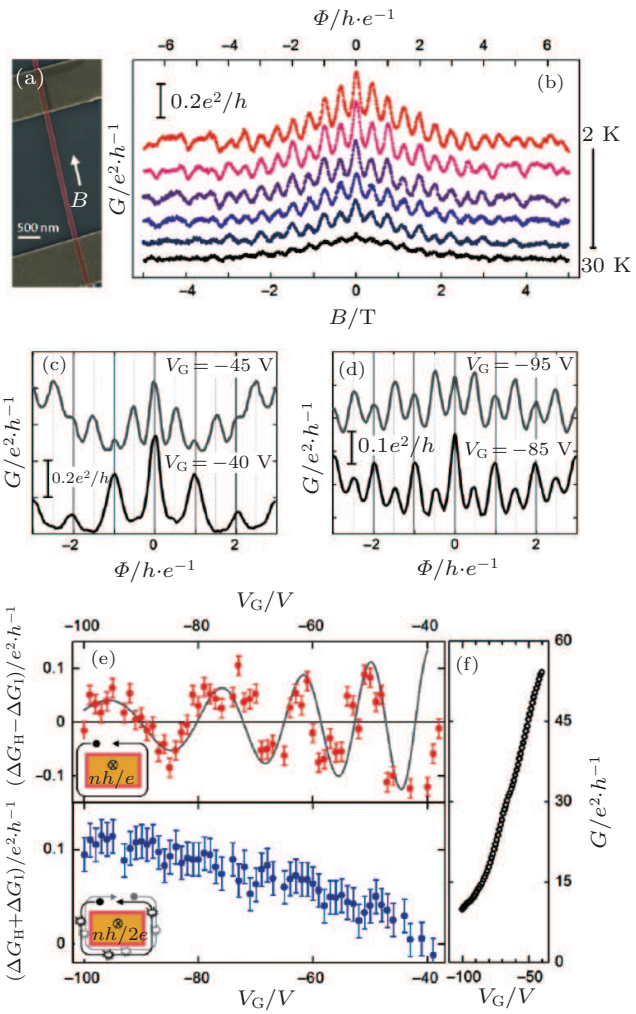


Fig. 7. Quantum oscillations in the longitudinal resistance of a Bi_2Se_3 nanowire with magnetic field applied parallel to the nanowire. (a) Scanning electron microscope image of the nanowire device equipped with an SiO_2/Si bottom gate. (b) Magnetotransport traces at several temperatures (T = 2–30 K). (c) and (d) The oscillations with h/e and $h/2e$ periodicities at several gate voltages. (e) Gate-voltage dependencies of the h/e-period and $h/2e$ oscillations. Here ΔG_H and ΔG_I are the amplitudes of conductance peak at the half flux quantum and integer flux quantum, respectively. (f) Gate-voltage dependence of the zero-field conductance.[102]

4. Summary and outlook

We have shown that there are remarkable experimental progresses in the field of 3D topological insulators. The improvements in the material quality and electrostatic gating ca-

pability have made the transport in the topological regime accessible in structures with various dimensions, including bulk single crystals, thin films, and nanoribbons. These advances paved the way for recent observation of the quantum anomalous Hall effect, a remarkable manifestation of dissipationless 1D edge states in magnetically doped TI thin films.[3] Nevertheless, most of predicted exotic quantum phenomena in TI and their hybrid structures with other materials still remain to be observed. To this end, it is necessary to further improve the quality of materials and gate-tuning capability, especially for the observation of the fragile quantum states associated with topological insulators.

Three-dimensional TI materials with truly insulating bulk are still out of reach for most experimental groups. Recent reports on strained HgTe epilayer[104] and SmB_6 single crystals[105–108] provide promising host materials for observing quantum phenomena that have stringent requirement of insulating bulk. However, further work on these materials is needed in order to confirm that they do have the anticipated topological order. Finally, as mentioned above, all of existing techniques for detecting the surface state transport have some limitations and sometimes they give inconsistent results. In thin films, there is also difficulty in evaluation of the residue bulk conductivity and its impact on the surface state properties. Therefore, novel methods for detecting weak bulk conductivity and its coupling to surface states[93] will be valuable to move this exciting field forward.

Acknowledgment

We are grateful to Jun Chen, Tong Guan, Xiaoyue He, Huajun Qin, Junren Shi, Xincheng Xie, Guanhua Zhang, and in particular Kehui Wu for fruitful collaborations. We thank Dimi Cucler, Xi Dai, Zhong Fang, Igor Gornyi, Ke He, Xucun Ma, Alexander Mirlin, Pavel Ostrovsky, Jurgen Smet, Yayu Wang, Peng Xiong, and Yugui Yao for stimulating discussions. We acknowledge valuable support from the Laboratory of Microfabrication at the Institute of Physics, Chinese Academy of Sciences.

References

[1] Von Klitzing K, Dorda G and Pepper M 1980 *Phys. Rev. Lett.* **45** 494
[2] König M, Wiedmann S, Brüne C, Roth A, Buhmann H, Molenkamp L W, Qi X L and Zhang S C 2007 *Science* **318** 766
[3] Chang C Z, Zhang J S, Feng X, *et al*. 2013 *Science* **340** 167
[4] Ohno H, Chiba D, Matsukura F, Omiya T, Abe E, Dietl T, Ohno Y and Ohtani K 2000 *Nature* **408** 944
[5] Koo H C, Kwon J H, Eom J, Chang J, Han S H and Johnson M 2009 *Science* **325** 1515
[6] Caviglia A D, Gariglio S, Reyren N, Jaccard D, Schneider T, Gabay M, Thiel S, Hammerl G, Mannhart J and Triscone J M 2008 *Nature* **456** 624
[7] Li Y Q and Smet J H 2008 *Spin Physics in Semiconductors* (Springer Berlin: M. I. Dyakonov)
[8] Fu L, Kane C L and Mele E J 2007 *Phys. Rev. Lett.* **98** 106803
[9] Moore J E and Balents L 2007 *Phys. Rev. B* **75** 121306
[10] Roy R 2009 *Phys. Rev. B* **79** 195322
[11] Fu L and Kane C L 2007 *Phys. Rev. B* **76** 045302
[12] Hsieh D, Qian D, Wray L, Xia Y, Hor Y S, Cava R J and Hasan M Z 2008 *Nature* **452** 970
[13] Hasan M Z and Kane C L 2010 *Rev. Mod. Phys.* **82** 3045
[14] Qi X L and Zhang S C 2011 *Rev. Mod. Phys.* **83** 1057
[15] Fu L and Kane C L 2008 *Phys. Rev. Lett.* **100** 096407
[16] Garate I and Franz M 2010 *Phys. Rev. Lett.* **104** 146802
[17] Zhang H J, Liu C X, Qi X L, Dai X, Fang Z and Zhang S C 2009 *Nat. Phys.* **5** 438
[18] Xia Y, Qian D, Hsieh D, Wray L, Pal A, Lin H, Bansil A, Grauer D, Hor Y S, Cava R J and Hasan M Z 2009 *Nat. Phys.* **5** 398
[19] Chen Y L, Analytis J G, Chu J H, Liu Z K, Mo S K, Qi X L, Zhang H J, Lu D H, Dai X, Fang Z, Zhang S C, Fisher I R, Hussain Z and Shen Z X 2009 *Science* **325** 178
[20] Butch N P, Kirshenbaum K, Syers P, Sushkov A B, Jenkins G S, Drew H D and Paglione J 2010 *Phys. Rev. B* **81** 241301
[21] Analytis J G, Chu J H, Chen Y L, Corredor F, McDonald R D, Shen Z X and Fisher I R 2010 *Phys. Rev. B* **81** 205407
[22] Kong D S, Cha J J, Lai K J, Peng H, Analytis J G, Meister S, Chen Y L, Zhang H J, Fisher I R, Shen Z X and Cui Y 2011 *ACS Nano* **5** 4698
[23] Hor Y S, Richardella A, Roushan P, Xia Y, Checkelsky J G, Yazdani A, Hasan M Z, Ong N P and Cava R J 2009 *Phys. Rev. B* **79** 195208
[24] Analytis J G, McDonald R D, Riggs S C, Chu J H, Boebinger G S and Fisher I R 2010 *Nat. Phys.* **6** 960
[25] Ren Z, Taskin A A, Sasaki S, Segawa K and Ando Y 2010 *Phys. Rev. B* **82** 241306
[26] Jia S, Ji H, Climent-Pascual E, Fuccillo M K, Charles M E, Xiong J, Ong N P and Cava R J 2011 *Phys. Rev. B* **84** 235206
[27] Zhang J S, Chang C Z, Zhang Z C, Wen J, Feng X, Li K, Liu M H, He K, Wang L L, Chen X, Xue Q K, Ma X C andWang Y Y 2011 *Nat. Commun.* **2** 574
[28] Kong D S, Chen Y L, Cha J J, Zhang Q F, Analytis J G, Lai K J, Liu Z K, Hong S S, Koski K J, Mo S K, Hussain Z, Fisher I R, Shen Z X and Cui Y 2011 *Nat. Nanotechnol.* **6** 705
[29] Taskin A A, Ren Z, Sasaki S, Segawa K and Ando Y 2011 *Phys. Rev. Lett.* **107** 016801
[30] Ren Z, Taskin A A, Sasaki S, Segawa K and Ando Y 2012 *Phys. Rev. B* **85** 155301
[31] Chen J, Qin H J, Yang F, Liu J, Guan T, Qu F M, Zhang G H, Shi J R, Xie X C, Yang C L, Wu K H, Li Y Q and Lu L 2010 *Phys. Rev. Lett.* **105** 176602
[32] Checkelsky J G, Hor Y S, Cava R J and Ong N P 2011 *Phys. Rev. Lett.* **106** 196801
[33] Yuan H T, Liu H W, Shimotani H, Guo H, Chen M W, Xue Q K and Iwasa Y 2011 *Nano Lett.* **11** 2601
[34] Kim D, Cho S, Butch N P, Syers P, Kirshenbaum K, Adam S, Paglione J and Fuhrer M S 2012 *Nat. Phys.* **8** 459
[35] He X Y, Guan T, Wang X X, Feng B J, Cheng P, Chen L, Li Y Q and Wu K H 2012 *Appl. Phys. Lett.* **101** 123111
[36] Culcer D 2012 *Physica E* **44** 860
[37] Bardarson J H and Moore J E 2013 *Rep. Prog. Phys.* **76** 056501
[38] Ando Y 2013 arXiv: 1304.5693 [cond-mat.mtrl-sci]
[39] Chen C Y, He S L, Weng H M and Zhou X J *et al*. 2012 *Proc. Nat. Acad. Sci.* **109** 3694
[40] Wrayer L A, Xu X Y, Xia Y, Hsieh D, Fedorov A V, Hor Y S, Cava R J, Bansil A, Lin H and Hasan M Z 2011 *Nat. Phys.* **7** 32
[41] Geim A K and Novoselov K S 2007 *Nat. Mater.* **6** 183
[42] Chen J 2012 *Electron Transport Properties of Topological Insulator Tuned with a Back-gate* (Ph.D Dissertation) (Beijing: Institute of Physics, Chinese Academy of Sciences) (in Chinese)
[43] Zhang T, Levy N, Ha J, Kuk Y and Stroscio J A 2013 *Phys. Rev. B* **87** 115410
[44] Zhang G H, Qin H J, Chen J, He X Y, Lv L, Li Y Q and Wu K H 2011 *Adv. Func. Mater.* **21** 2351
[45] Nevilla R C, Hoeneisen B and Mead C A 1972 *J. Appl. Phys.* **43** 2124
[46] Yang W M, Lu Z G and Li Y Q to be published
[47] Steinberg H, Gardner D R, Lee Y S and Jarillo-Herrero P 2010 *Nano Lett.* **10** 5032
[48] Sacëpë B, Ostinga J B, Li J, Ubaldini A, Couto N J G, Giannini E and Morpurgo A F 2010 *Nat. Commun.* **2** 575
[49] Kong D S, Dang W H, Cha J J, Li H, Meister S, Peng H L, Liu Z F and Cui Y 2010 *Nano Lett.* **10** 2245

[50] Coletti C, Riedl C, Lee D S, Krauss B, Patthey L, von Klitzing K, Smet J H and Starke U 2010 *Phys. Rev. B* **81** 235401

[51] Cho S, Dellabetta B, Yang A, Schneeloch J, Xu Z J, Valla T, Gu G, Gilbert M J and Mason N 2013 *Nat. Commun.* **4** 1689

[52] Xiu F, He L A, Wang Y, Cheng L, Chang L T, Lang M, Huang G, Kou X, Zhou Y, Jiang X W, Chen Z Q, Zou J, Shailos A and Wang K L 2011 *Nat. Nanotech.* **6** 216

[53] Chiu S P and Lin J J 2013 *Phys. Rev. B* **87** 035122

[54] Cha J J, Kong D S, Hong S S, Analytis J G, Lai K J and Cui Y 2012 *Nano Lett.* **12** 1107

[55] Gehring P, Gao B, Burghard M and Kern K 2012 *Appl. Phys. Lett.* **101** 023116

[56] Hong S S, Cha J J, Kong D S and Cui Y 2012 *Nat. Commun.* **3** 757

[57] Xia B, Ren P, Sulaev A, Liu P, Shen S Q and Wang L 2013 *Phys. Rev. B* **87** 085442

[58] Lang M, He L, Kou X F, Upadhyaya P, Fan Y, Chu H, Jiang Y, Bardarson J H, Jiang W J, Choi E S, Wang Y, Yeh N C, Moore J and Wang K L 2013 *Nano Lett.* **13** 48

[59] Lee J, Park J, Lee J H, Kim J S and Lee H J 2012 *Phys. Rev. B* **86** 245321

[60] Steinberg H, Laloë J B, Fatemi V, Moodera J S and Jarillo-Herrero P 2011 *Phys. Rev. B* **84** 233101

[61] Liao J *et al*. to be published

[62] Wang J, Chen X, Zhu B F and Zhang S C 2012 *Phys. Rev. B* **85** 235131

[63] Dhoot A S, Yuen J D, Heeney M, McCulloch I, Moses D and Heeger A J 2006 *Proc. Natl. Acad. Sci. USA* **103** 11834

[64] Panzer M J and Frisbie C D 2006 *Adv. Funct. Mater.* **16** 1051

[65] Ueno K, Nakamura S, Shimotani H, Ohtomo A, Kimura N, Nojima T, Aoki H, Iwasa Y and Kawasaki M 2008 *Nat. Mater.* **7** 855

[66] Yuan H T, Liu H W, Shimotani H, Guo H, Chen M, Xue Q K and Iwasa Y 2011 *Nano Lett.* **11** 2601

[67] Shimizu S, Yoshimi R, Hatano1 T, Takahashi K S, Tsukazaki A, Kawasaki M, Iwasa Y and Tokura Y 2012 *Phys. Rev. B* **86** 045319

[68] Segawa K, Ren Z, Sasaki S, Tsuda T, Kuwabata S and Ando Y 2012 *Phys. Rev. B* **86** 075306

[69] Bianchi M, Guan D, Bao S, Mi J, Iversen B B, King P D C and Philip H 2010 *Nat. Commun.* **1** 128

[70] Hsieh D, Xia Y, Wray L, Qian D, Pal A, Dil J H, Osterwalder J, Meier F, Bihlmayer G, Kane C L, Hor Y S, Cava R J and Hasan M Z 2009 *Science* **323** 919

[71] Schoenberg D 1984 *Magnetic Oscillations in Metals* (Cambridge: Cambridge University Press)

[72] Köhler H 1973 *Phys. Stat. Sol. B* **58** 91

[73] Taskin A A, Segawa K and Ando Y 2010 *Phys. Rev. B* **82** 121302

[74] Qu D X, Hor Y S, Xiong J, Cava R J and Ong N P 2010 *Science* **329** 821

[75] Analytis J G, McDonald R D, Riggs S C, Chu J H, Boebinger G S and Fisher I R 2010 *Nat. Phys.* **6** 960

[76] Mikitik G P and Sharlai Y V 1999 *Phys. Rev. Lett.* **82** 2147

[77] Novoselov K S, Geim A K, Morozov S V, Jiang D, Katsnelson M I, Grigorieva I V, Dubonos S V and Firsov A A 2005 *Nature* **438** 197

[78] Zhang S Y, Tan W, Stormer H L and Kim P 2005 *Nature* **438** 201

[79] Xiong J, Luo Y K, Khool Y, Cava R J and Ong N P 2012 *Phys. Rev. B* **86** 045314

[80] Wright A R and McKenzie R H 2013 *Phys. Rev. B* **87** 085411

[81] Xiong J, Perersen A C, Cava R J and Ong N P 2012 *Physica E* **44** 917

[82] Bansal N, Kim Y S, Brahlek M, Edrey E and Oh S 2012 *Phys. Rev. Lett.* **109** 116804

[83] Zhang S X, McDonald R D, Shekhter A, Bi Z X, Li Y, Jia Q X and Picraux S T 2012 *Appl. Phys. Lett.* **101** 202403

[84] Assaf B A, Cardinal T, Wei P, Katmis F, Moodera J S and Heiman D 2013 *Appl. Phys. Lett.* **102** 012102

[85] Wang X L, Du Y, Dou S X and Zhang C 2012 *Phys. Rev. Lett.* **108** 266806

[86] Bergmann G 1984 *Phys. Rep.* **107** 1

[87] Ando T, Nakanishi T and Saito R 1998 *J. Phys. Soc. Jpn.* **67** 2857

[88] Li Y Q, Wu K H, Shi J R and Xie X C 2012 *Front. Phys.* **7** 165

[89] Chen J, He X Y, Wu K H, Ji Z Q, Lu L, Shi J R, Smet J H and Li Y Q 2011 *Phys. Rev. B* **83** 241304

[90] Garate I and Glazman L 2012 *Phys. Rev. B* **86** 035422

[91] Kim D, Syers P, Butch N P and Fuhrer S 2013 *Nat. Commun.* **4** 2040

[92] Yu X X, He L, Lang M, Jiang W J, Xiu F, Liao Z, Wang Y, Kou X F, Zhang P, Tang J, Huang G, Zou J and Wang K L 2013 *Nanotechnology* **24** 015705

[93] Lin C J, He X Y, Liao J, Wang X X, Sacksteder IV V, Yang W M, Guan T, Zhang Q M, Gu L, Zhang G Y, Zeng C G, Dai X, Wu K H and Li Y Q 2013 *Phys. Rev. B* **88** 041307

[94] Altshuler B L, Aronov A G and Spivak B Z 1981 *JETP Lett.* **33** 94

[95] Sharvin D Y and Sharvin Y V 1982 *JETP Lett.* **34** 272

[96] Bachtold A, Strunk C, Salvetat J P, Bonard J M, Forrö L, Nussbaumer T and Schönenberger C 1999 *Nature* **397** 673

[97] Bardarson J H, Brouwer P W and Moore J E 2010 *Phys. Rev. Lett.* **105** 156803

[98] Zhang Y and Vishwanath A 2010 *Phys. Rev. Lett.* **105** 206601

[99] Peng H L, Lai K J, Kong D, Meister S, Chen Y L, Qi X L, Zhang S C, Shen Z X and Cui Y 2010 *Nat. Mater.* **9** 225

[100] Li Z G, Qin Y Y, Song F Q, Wang Q H, Wang X F, Wang B G, Ding H F, Van Haesondonck C, Wan J G, Zhang Y H and Wang G H 2012 *Appl. Phys. Lett.* **100** 083107

[101] Tian M L, Ning W, Qu Z, Du H F, Wang J and Zhang Y H 2013 *Sci. Rep.* **3** 1212

[102] Sulaev A, Ren P, Xia B, Lin Q H, Yu T, Qiu C, Zhang S Y, Han M Y, Li Z P, Zhu W G, Wu Q Y, Feng Y P, Shen L, Shen S Q and Wang L 2013 *AIP Advances* **3** 032123

[103] Hong S S, Zhang Y, Cha J J, Qi X L and Cui Y 2013 arXiv: 1303.1601 [cond-mat.mes-hall]

[104] Brüne C, Liu C X and Shen Z X 2011 *Phys. Rev. Lett.* **106** 126803

[105] Dzero M, Sun K, Galitski V and Coleman P 2010 *Phys. Rev. Lett.* **104** 106408

[106] Wolgast S, Kurdak C, Sun K, Allen J W, Kim D J and Fisk Z 2012 arXiv: 1211.5104 [cond-mat.str-el]

[107] Zhang X H, Butch N P, Syers P and Paglione J 2013 *Phys. Rev. X* **3** 011011

[108] Lu F, Zhao J Z, Weng H M, Fang Z and Dai X 2013 *Phys. Rev. Lett.* **110** 096401